

1 **Characterization of the mesostructural organization of cement particles in**
2 **fresh cement paste**

3
4 Zhang Yanrong¹, Kong Xiangming^{2*}, Gao Liang^{3*}, Bai Yun⁴

5 ¹ School of Civil Engineering, Beijing Key Laboratory of Track Engineering, Beijing Jiaotong
6 University, Beijing, 100044, China

7 ² Department of Civil Engineering, Tsinghua University, Beijing, 100084, China

8 ³ Beijing Engineering and Technology Research Center of Rail Transit Line Safety and
9 Disaster Prevention, Beijing Jiaotong University, Beijing, 100044, China

10 ⁴ Department of Civil, Environmental and Geomatic Engineering, University College London,
11 Gower Street, WC1E 6BT, London, UK

12
13 Correspondence to: Kong Xiangming and Gao Liang

14 (Tel.: +86-10-58687244, Email: kxm@tsinghua.edu.cn

15 Tel.: +86-10-58687243, Email: gaol@bjtu.edu.cn)

16
17 **Abstract:** Comparative study on the mesostructures of fresh cement paste (FCP) in different
18 dispersion mediums was carried out aiming at characterizing the structural organization of
19 cement particles in FCP at a mesoscopic scale and establishing the correlation of
20 mesostructure with rheological properties. For the first time, Morphologi G3 was adopted to
21 *in-situ* characterize the mesostructure of FCP. Several dispersion mediums including air,

22 deionized water, ethanol and an aqueous solution of ethanol were chosen to study the
23 dispersion of cement particles in the selected mediums. Superplasticizers, as dispersing aids
24 for cement particles, were added to change the dispersion of cement particles. Results show
25 that Morphologi G3 with the high sensitivity and the high resolution is a powerful tool for *in-*
26 *situ* characterization of the mesostructure of FCP by providing high-quality images
27 associated with structural parameters. The structural parameters including particle size,
28 circularity and fractal dimension of particle spatial distribution (Dpd) allow to quantitatively
29 characterize the organization of cement particles in FCP at a mesoscopic scale, through
30 which the relationship between the mesostructure and the rheological behavior of FCP was
31 established. Higher fluidity signifies larger Dpd and circularity but a lower mean particle size.
32 Moreover, the mean particle size and Dpd are more sensitive to indicate the fluidity change.

33

34 **Key words:** Characterization; Mesostructure; Fresh cement paste; Superplasticizers;
35 Rheology

36

37 **1. Introduction**

38 Workability of cementitious materials has drawn considerable attentions due to its essential
39 role in the construction process as well as the important impacts on the mechanical properties
40 and even the durability of hardened concrete. Extensive research has been carried out on
41 the workability by measuring the rheological properties, viscoelastic properties and thixotropy
42 of fresh cementitious materials [1–3]. From the microscopic point of view, all these

43 macroscopic properties of fresh cementitious mixtures are primarily determined by the
44 microscopic structures, e.g. the packing or dispersion state of cement particles in the
45 suspension systems [4–6]. It has been widely realized that agglomeration of cement particles
46 immediately takes places upon the contact of cement to water, which originates from the
47 minimization of the interfacial energy between cement and the dispersion medium, usually
48 water, and from the basically electrostatic interaction between cement particles [7, 8].
49 Superplasticizers are practically used to achieve higher fluidity of fresh cement paste (FCP).
50 The working mechanism of superplasticizers is to facilitate the dispersion of cement particles
51 by generating the so-called steric and/or electrostatic repulsion between cement particles [6,
52 9–11]. Thus, the desired fluidity could be achieved by properly modifying the microstructure
53 of the paste, namely by the enhanced dispersion of cement particles. This stimulated the
54 interest of many researchers to investigate the microstructure of FCP as well as its correlation
55 with the macroscopic rheological properties.

56

57 The observation of FCP by microscopes is a direct way to analyze the microstructure of the
58 FCP. Much research has been dedicated to studying the structural organization of cement
59 particles in FCP as well as its time dependent evolution based on microscopy and
60 granulometry techniques [12–19]. Optical and scanning electron microscopes have been
61 frequently used to observe the mesostructure of a diluted FCP focusing on the granular
62 shape and surface as well as the flocculation [12–15]. Analysis of the microscopic images by
63 image processing software enables us to obtain the quantitative information of different

64 granular populations like the shape index, size distribution and so on [15–18]. However, the
65 obtained information is far from being satisfied due to the low resolution and the limited
66 measuring area of a regular microscope. Furthermore, laser granulometry has also been
67 applied in the quantitative analysis of the mesostructure of cement paste [15, 19]. Autier [15]
68 characterized the dispersion state of cement particles by using a morpho-granulometric
69 approach based on the complementarity of scanning electron microscopy and laser
70 granulometry, in which dispersion indices were introduced to characterize the mesostructural
71 variation caused by the inclusion of superplasticizers. However, it was found that the particle
72 size results provided by laser granulometry do not well correspond to the images presented
73 in SEM, i.e., some agglomerates appeared in the particle size distribution curve were not
74 observed in microscopy. Meanwhile, the dispersion indices could be used to identify the
75 influence of the superplasticizers but not the influence of molecular structure. The different
76 influences of the molecular structure were distinguished by an indirect characterization
77 approach of mesostructural organization in term of behavior settling (Phase separation Index)
78 [20]. Wang [21] considered cement paste as a Menger sponge with fractal structure and
79 figured out the fractal dimension of particle size distribution to quantitatively characterize the
80 flocculated structures. But it did not present evident variations when different dosages of
81 superplasticizers were added into the paste. It is supposed that there must miss some vital
82 information in the case of characterizing the microstructure using dispersion indices or
83 particle size fractal dimension.

84

85 In spite of some efforts put on this topic, quantitative characterization on the mesostructure
86 of FCP remains a challenge and accordingly the clear correlation of mesostructure with
87 rheological behaviors of FCP has not been established. In this study, Morphologi G3 with
88 high sensitivity and resolution was employed to systematically explore the mesostructure of
89 diluted FCPs with the aim of quantitatively characterizing the structural organization of
90 cement particles in FCP at a mesoscopic scale and establishing the correlation of
91 mesostructure with macroscopic rheological properties.

92

93 As the first step, different structural organization of cement particles were identified in
94 reference cement pastes with different dispersion mediums like air, deionized water, ethanol
95 and an aqueous solution of ethanol. Structural parameters including particle size distribution,
96 shape index and fractal dimension of particle spatial distribution were obtained on the basis
97 of tens to hundreds of thousands of particles to characterize the mesostructure of FCP. In
98 addition, two types of superplasticizers were added into the cement pastes to investigate the
99 sensitivity of the selected structural parameters to the change of the dispersion states of the
100 cement particles that is caused by the addition of the superplasticizers. Relying on the three
101 structural parameters, we established the relationship between the mesostructural
102 organization of cement particles in a fresh cement paste and its rheological behavior. This
103 research allows us to have a better understanding of the influence of superplasticizers
104 (amount, type i.e. PCE and NSF) on the rheological behavior of a cement pastes and may
105 provide theoretical guidance for adjusting workability of FCP.

106

107 2. Experimental

108 2.1. Materials and sample preparation

109 2.1.1. Materials

110 Reference cement P·I 42.5 with the fineness of 2.3% and the density of 3.10 g·cm⁻³ was
111 used in this study, which was provided by China Building Materials Academy and complies
112 with the Chinese standard GB8076-2008. The composition of the cement is listed in Table 1.

113 Table 1 Chemical and mineral composition of cement

Chemical composition (wt %)										Mineral composition (wt %)			
SiO ₂	Al ₂ O ₃	Fe ₂ O ₃	CaO	MgO	SO ₃	Na ₂ O _{eq}	f-CaO	Loss	Cl ⁻	C ₃ S	C ₂ S	C ₄ AF	C ₃ A
21.58	4.03	3.46	61.49	2.60	2.83	0.51	0.67	1.97	0.010	57.34	18.90	11.25	6.47

114

115 A self-synthesized polycarboxylate (PCE) type superplasticizer with solid content of 40 wt.%
116 was employed, which is an aqueous solution of copolymer of acrylic acid, methyl
117 polyethylene glycol methacrylate and 2-acrylamido-2-methylpropane sulfonic acid with
118 number average molecular weight M_n of 3.662×10^4 and polydispersity index M_w/M_n of 2.48.

119 A commercial naphthalene sulfonate formaldehyde (NSF) type superplasticizer was provided
120 by Huadi Synthetic Material Co. Ltd.

121

122 Analytical grade of ethanol absolute (>99.7% purity) and deionized water were employed.

123

124 2.1.2. Sample preparation and measurements

125 2.1.2.1. Mesostructure characterization of fresh cement pastes

126 Microfabric of rock and soil materials usually consists of morphological characteristics,
127 geometric characteristics and energy characteristics, and could be described by some
128 structural factors such as granular morphology, contact relation, orientation and porosity etc
129 [22–24]. Furthermore, a structural feature could be characterized quantitatively by one or
130 several structural parameters. Fresh cement paste is generally considered as a suspension
131 system and its mesostructure may also be characterized by this approach based on several
132 structural parameters. In this study, special attentions were paid to the structural factors
133 including granular morphology, granular agglomerates and the spatial distribution of particles.
134 Three corresponding structural parameters, particle size, granular shape and fractal
135 dimension of particle spatial distribution (D_{pd}), were extracted from the image analysis to
136 quantitatively characterize the mesostructure of diluted fresh cement paste.

137

138 A high sensitivity and high resolution analytical tool Morphologi G3 (Malvern Instruments
139 Limited, Malvern, UK) was employed to characterize the mesostructure of diluted FCP. The
140 instrument captures the image of each particle by scanning the sample underneath the
141 microscope optics, while keeping the particles in focus. Advanced graphing and data
142 classification options in the software ensure that the extracted relevant data concerning the
143 morphological properties for each particle from the measurement is as straightforward as
144 possible, via an intuitive visual interface.

Table 2 Formulation of the diluted cement suspension samples

Sample No.	Dispersed phase	Dispersion medium	E/C ^a	W/C ^b	Superplasticizer concentration
C-A	Cement	Air	0	0	0
C-E	Cement	Ethanol	200	0	0
C-W	Cement	Water	0	200	0
C-EW	Cement	Ethanol solution	100	100	0
C-E+C-W	Cement	Ethanol and water	200	200	0
C-W-P0.1	Cement	Water+ PCE superplasticizer	0	200	0.1%
C-W-P0.3	Cement	Water+ PCE superplasticizer	0	200	0.3%
C-W-P0.5	Cement	Water+ PCE superplasticizer	0	200	0.5%
C-W-N0.5	Cement	Water+ NSF superplasticizer	0	200	0.5%

146 ^a denotes the mass ratio of ethanol to cement.

147 ^b means the mass ratio of water to cement in C-W, C-EW and C-E+C-W system while
 148 indicates the mass ratio of superplasticizer solution to cement in the C-W-P and C-W-N
 149 system.

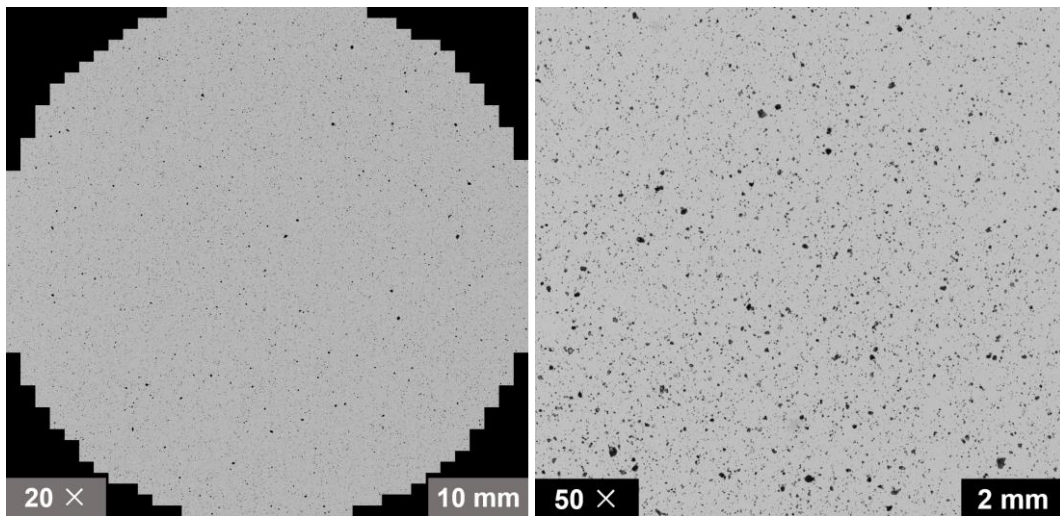
150

151 The cement suspension samples with different dispersion mediums were prepared according
 152 to the formulations shown in Table 2. 1) C-A system: a small amount of cement powder was
 153 dispersed on a stage using an integrated dry powder disperser with an air pressure of 200
 154 and 500 kPa. 2) C-E system or C-W system: cement powder was introduced into deionized

155 water or ethanol with the mass ratio of 1:200, and then was mixed at a speed of 125 rpm for
156 2 minutes. After a 10 sec interval, mixing was resumed for an additional 2 min at 125 rpm. 3)
157 C-EW system: an aqueous solution of ethanol was prepared with mass ratio of ethanol to
158 water of 1:1 and then cement powder was introduced into the solution with mass ratio of
159 1:200. They were mixed according to the above procedure. 4) C-E+C-W system: equal mass
160 of C-E mixture and C-W mixture were taken and mixed well. 5) C-W-P system: three aqueous
161 solutions with PCE mass concentration of 0.1%, 0.3% and 0.5% as well as an aqueous
162 solution with NSF mass concentration of 0.5% were prepared, and then cement powder was
163 introduced to the solutions with mass ratio of 1:200 and mixed well.

164

165 The well-mixed cement suspension of 2 mL was taken and injected into a wet cell. The
166 dispersed cement powder on the stage as well as the suspension in the wet cell was instantly
167 subjected to observation by Morphologi G3. In the meantime of scanning the particles, the
168 high-quality image of each particle was captured and a 2-dimensional projection using
169 geometrical calculations was performed on these collected images. Finally, apart from a
170 global picture containing all the scanned particles as shown in Fig. 1, the structural
171 parameters, particle size and shape as well as fractal dimension of spatial distribution, were
172 constructed on the basis of the tens to hundreds of thousands of particles. The whole process
173 including sample preparation and analysis by Morphologi G3 lasted for 15 min. That is to say
174 that the effect of cement hydration within such a short period can be neglected in the case of
175 cement and water mixtures.



176

177

178

179

180

181

182

183

184

185

186

187

188

189

190

191

(a)

(b)

Fig. 1 Global images of samples by Morphologi G3

(a) C-A system; (b) C-W-P0.3 system

Cement particles are 3-dimensional objects with irregular shapes, thus they cannot be fully described by a single dimension such as a radius or diameter. In order to simplify the measurement process, the particle size is defined by the diameter of an equivalent circle (CE diameter) having an area the same as the particle image, which is different from the volume diameter measured by a laser granulometry. The particle shape is described by circularity, which is the ratio of the circumference of a circle equal to the projected area to the perimeter of the particle, and is calculated as:

$$C = \frac{2 \times \sqrt{\pi \times Area}}{Perimeter} \quad (1)$$

where Area is the projected area of the particle and perimeter is the perimeter of the particle.

Fractal dimension of particle distribution (Dpd) provides necessary information about the

192 distribution of particles in a 2-dimension image, i.e. the dispersion degree of particles, which
193 is defined based on the statistical analysis theory about mesh simplification on a 2-dimension
194 image.

$$195 \quad D_{pd} = - \lim_{\epsilon \rightarrow 0} \frac{\ln N(\epsilon)}{\ln \epsilon} \quad (2)$$

196 in which, ϵ and $N(\epsilon)$ are respectively the side length of the mesh and the amount of mesh
197 with side length of ϵ on the particle image. In this case, higher D_{pd} reflects larger dispersion
198 degree and vice versa.

199

200 2.1.2.2. Rheological tests

201 Mini-cone test is a simple and effective method to get a rough view on the rheological
202 properties of cementitious materials, which is represented by spread diameter. The spread
203 diameter result has been proved to be able to classify different materials in terms of their
204 ability to fill a formwork and is inversely proportional to the yield stress that is one of key
205 rheological parameters of FCP. In this study, a copper cone with top diameter of 36 mm,
206 bottom diameter of 60 mm and height of 60 mm was used.

207

208 The samples were prepared in accordance with the formulations in Table 3. The mass
209 solid/solid ratios of superplasticizers to cement varied from 0 to 0.5%. The mass ratio of water
210 to cement in all the cement pastes was fixed at 0.4, in which the water contained in the
211 superplasticizers was included. In the case of ethanol included as dispersion medium, the
212 total mass of water and ethanol was fixed at half of the mass of cement. Dispersion mediums

213 were firstly added into a mixer, and then cement powder was gradually introduced over a
 214 time span of 2 min into the mixer at 62 rpm. After a 10 sec interval, mixing was resumed for
 215 an additional 2 min at 125 rpm. The well-mixed fresh paste was poured into the cone right
 216 away and then, the cone was quickly lifted up. The average value of spread diameters of the
 217 FCP in varied dispersion mediums was recorded after the paste stopped flowing. It is noted
 218 that a slight bleeding phenomenon happened at Sp/C of 0.5% and hence the bleeding water
 219 ring surrounding the paste was excluded in the measurement of spread diameter.

220 Table 3 Formulation of the cement suspension samples

Sample No.	Dispersed phase	Dispersion Medium	E/C ^a	W/C ^b	Sp/C ^c
C-A	Cement	Air	0	0	0
C-E	Cement	Ethanol	0.4	0	0
C-W	Cement	Water	0	0.4	0
C-EW	Cement	Ethanol solution	0.2	0.2	0
C-E+C-W	Cement	Ethanol and water	0.4	0.4	0
C-W-P0.1	Cement	Water+ PCE superplasticizer	0	0.4	0.1%
C-W-P0.3	Cement	Water+ PCE superplasticizer	0	0.4	0.3%
C-W-P0.5	Cement	Water+ PCE superplasticizer	0	0.4	0.5%
C-W-N0.5	Cement	Water+ NSF superplasticizer	0	0.4	0.5%

221 ^a The mass ratio of ethanol to cement.

222 ^b The mass ratio of water to cement.

223 ^c The mass solid/solid ratios of superplasticizers to cement.

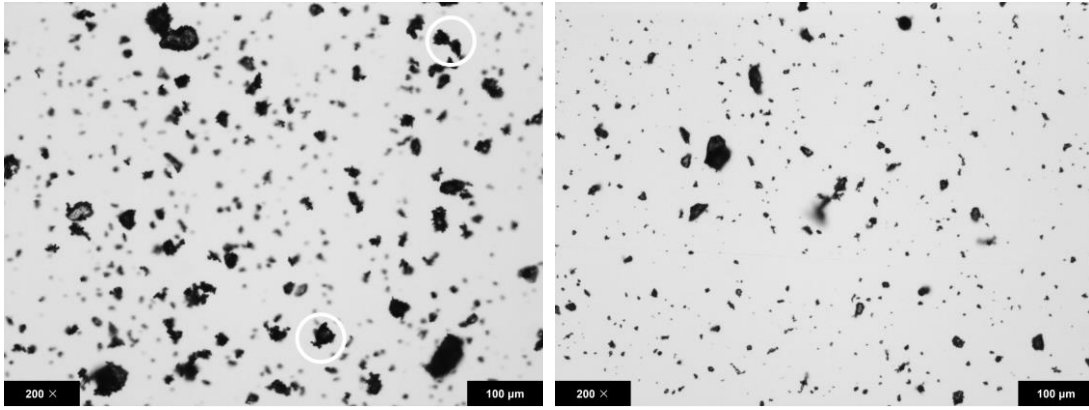
224 **3. Results and discussion**

225 3.1. Characteristics of cement particles in varied dispersion mediums without superplasticizer

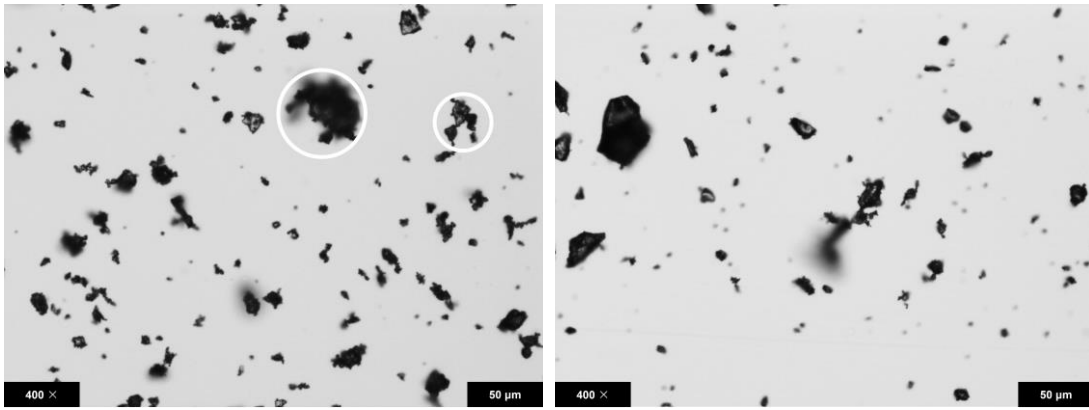
226 3.1.1. C-A system

227 The cement particles dispersed in air fluid are observed by Morphologi G3 as shown in Fig.
228 2, in which small particles (S) are the particles with size of 1-10 μm , medium particles (M)
229 indicate the particles of 10-30 μm and large particles (L) denote the particles with size of
230 larger than 30 μm . Separated cement particles with spinous edge as well as a large quantity
231 of loosely agglomerated cement particles are observed. The agglomerations of cement
232 particles are present in two modes: the association of small particles and the adhesion of
233 small particles on large particles, as circled in Fig. 2(a)-2(c). We define the structure of the
234 association of the small particles as S-S structure and the structure of the small particles
235 sticking to the larger ones as L-S structure. It is believed that the intrinsic charges on the
236 cement surface originating from the fracture of valence bond during the grinding procedure
237 of cement clinker are majorly responsible for the existence of agglomerates [25]. Moreover,
238 small particles usually present strong adhesive force (Van der Waals force) because of their
239 huge surface energy, and hence tend to form agglomerates more easily by associating with
240 each other or adhering on the surface of large particle. If the dispersion pressure is increased
241 to 500 kPa, the total amount of agglomerates significantly reduce as shown in Fig. 2(d)-2(f).
242 The particle size distribution of cement particles in air fluid from 1 to 100 μm is shown in Fig.
243 3, with a mean size of 4.98 μm . The circularity and Dpd of C-A system is 0.91 and 1.84,
244 respectively.

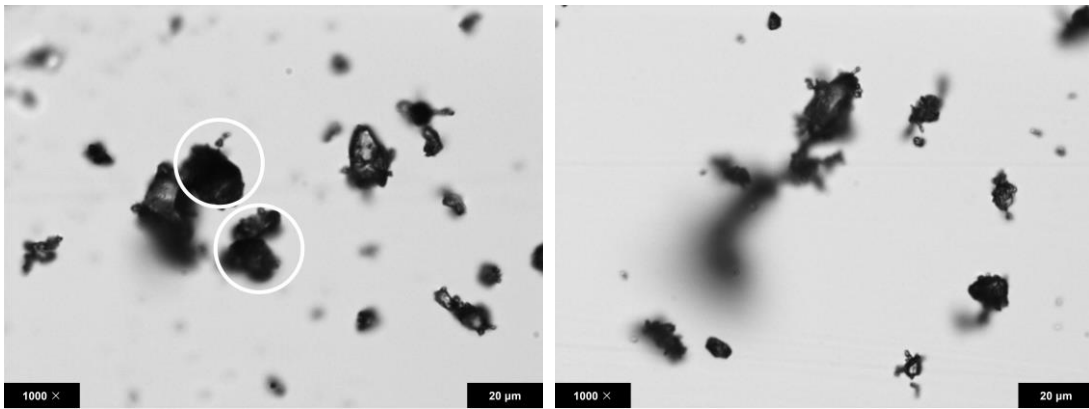
245
246



247
248

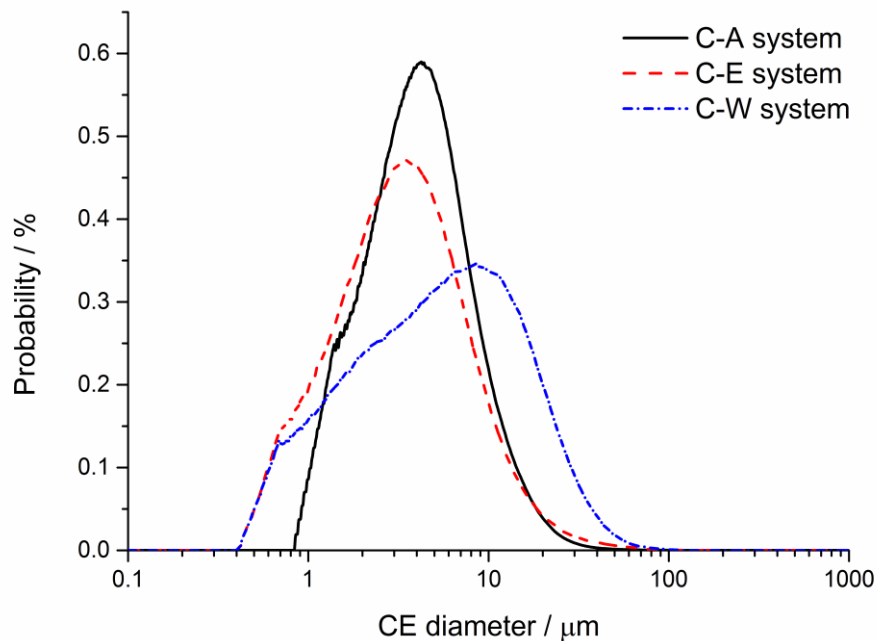


249
250



251
252
253

Fig. 2 Images of organization structure of cement particles in C-A system at different dispersed pressures (a)(b)(c) 200 kPa; (d)(e)(f) 500 kPa



254

255 Fig. 3 Particle size distribution of C-A, C-E and C-W systems

256

257 3.1.2. C-E and C-W systems

258 When cement powder is dispersed in ethanol, it has been well-understood that neither

259 dissolution of the mineral phases in cement nor any reaction between cement and ethanol

260 takes place in a short time range [15]. Thus, it can be assumed that the charges properties

261 of cement particles presenting in ethanol should be similar to those of cement dispersed in

262 air. The organization of cement particles in C-E system should be similar to that of C-A system,

263 i.e. the association of small particles (S-S structure) and the adhesion of small particles on

264 large particles (L-S structure). Surprisingly, it is found from Fig. 4(a)-4(c) that the cement

265 particles present majorly individual particles together with a small amount of association

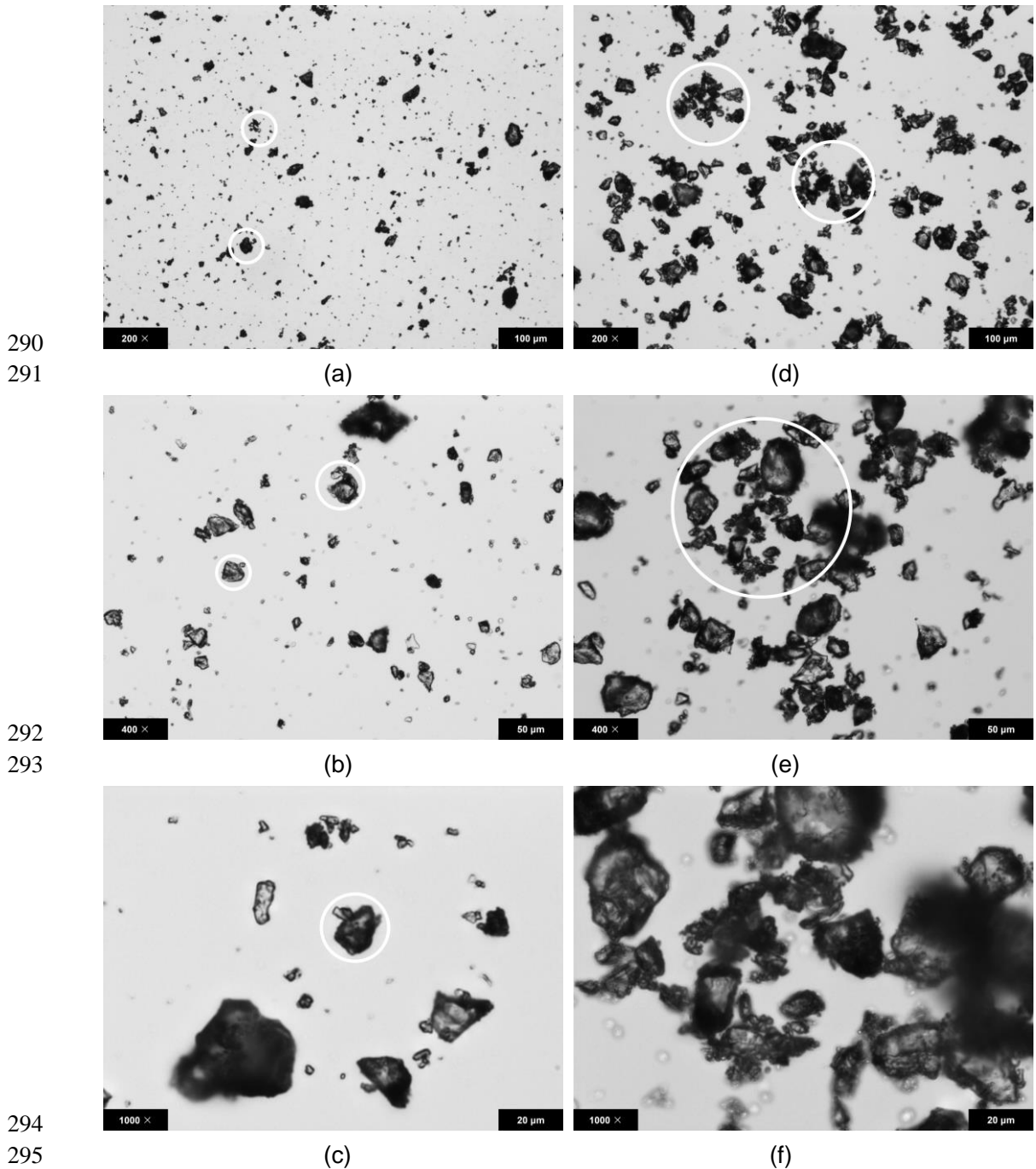
266 structure of L-S structures. That is to say, S-S structures, which abound in C-A system, are

267 rarely observed in C-E system. From this finding, we may propose that the formation of S-S
268 structure is mainly driven by the minimization of surface energy rather than by the
269 electrostatic interaction among particles. This driving force in C-E system is weaker than that
270 in C-A system because the interfacial energy between cement surface and ethanol is lower
271 than that between cement surface and air [26]. As a consequence, the cement particles
272 exhibit better dispersion in ethanol medium than in air. The mean particle size of C-E system
273 is 4.59 μm , which is slightly lower than that of C-A system due to the increased amount of
274 small particles as seen in Fig. 3. The circularity and Dpd of C-E system are 0.83 and 1.87,
275 respectively. These evidence the hypothesis that ethanol behaves as an inert and good
276 dispersion medium for cement particles [15].

277

278 On the contrary, once cement comes into contact with water, quick dissolution of mineral
279 phases as well as hydration starts immediately, which produces numerous positive and
280 negative charges on cement surface and hence strong electrostatic interactions among
281 cement particles that is believed to be much stronger than that in C-A or C-E system. The
282 strong electrostatic interaction may cause more intensive association of cement particles. It
283 is noted from Fig. 4(d)-4(f), cement particles of different sizes aggregate together and enwrap
284 much water, as circled in Fig. 4(d) and 4(e). The whole structure with blurry and spinous edge
285 exhibits irregular shape of vesicle and is called flocculated structure, which contains
286 agglomeration of cement particles with full range of size. The association of large particles,
287 L-L structure, which is absent in C-A and C-E systems, is produced mainly by the strong

288 electrostatic interactions among cement particles. That is to say, the dispersion of cement
289 particles in water is much worse than in the mediums of air and ethanol.



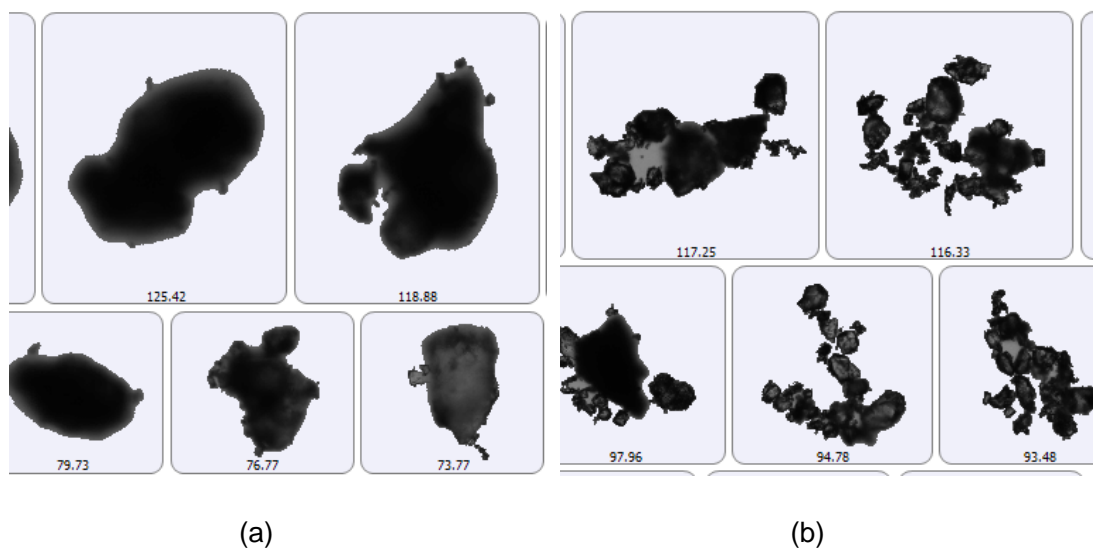
296 Fig. 4 Images of organization structure of cement particles in C-E system (a)(b)(c)and C-W
297 system (d)(e)(f)

298

299 As seen from Fig. 3, the particle size distribution of C-W system evidently differs from those
300 of C-A and C-E systems, in which the amount of the particles with size of larger than 20 μm
301 sharply rises. As a result, the mean particle size of C-W system increases to 8.09 μm . In
302 addition, the Dpd descends to 1.68, which demonstrates the dispersion degree of cement
303 particles in deionized water is very low.

304

305 A part of images of large particles captured by Morphologi G3 is exhibited in Fig. 5. The
306 abovementioned differences between C-E and C-W systems in term of granular morphology
307 could be distinctly noticed.



308

309

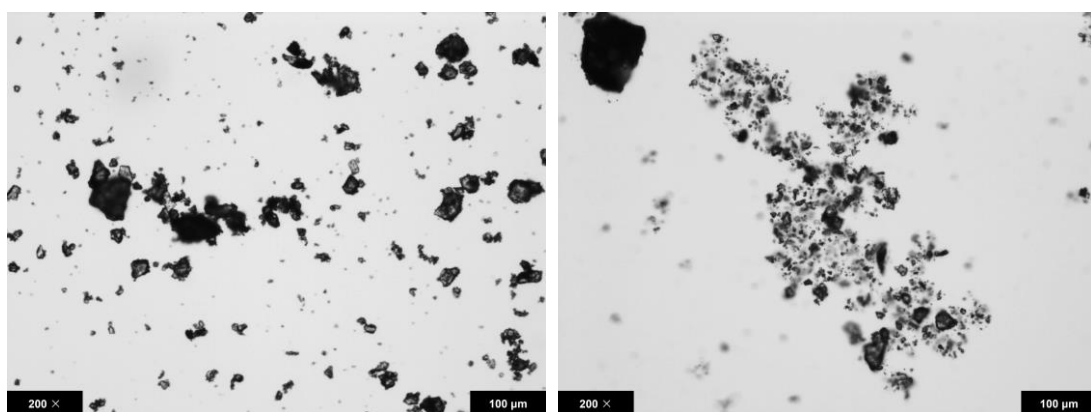
310 Fig. 5 Typical morphology and CE diameter of particles in C-E system (a) and C-W system
311 (b) (μm)

312

313 3.1.3. C-EW and C-E+C-W systems

314 Compared to the case of ethanol as the dispersion medium, when the aqueous solution of
315 ethanol is used as the dispersion medium for cement, it is expected that the water in solution

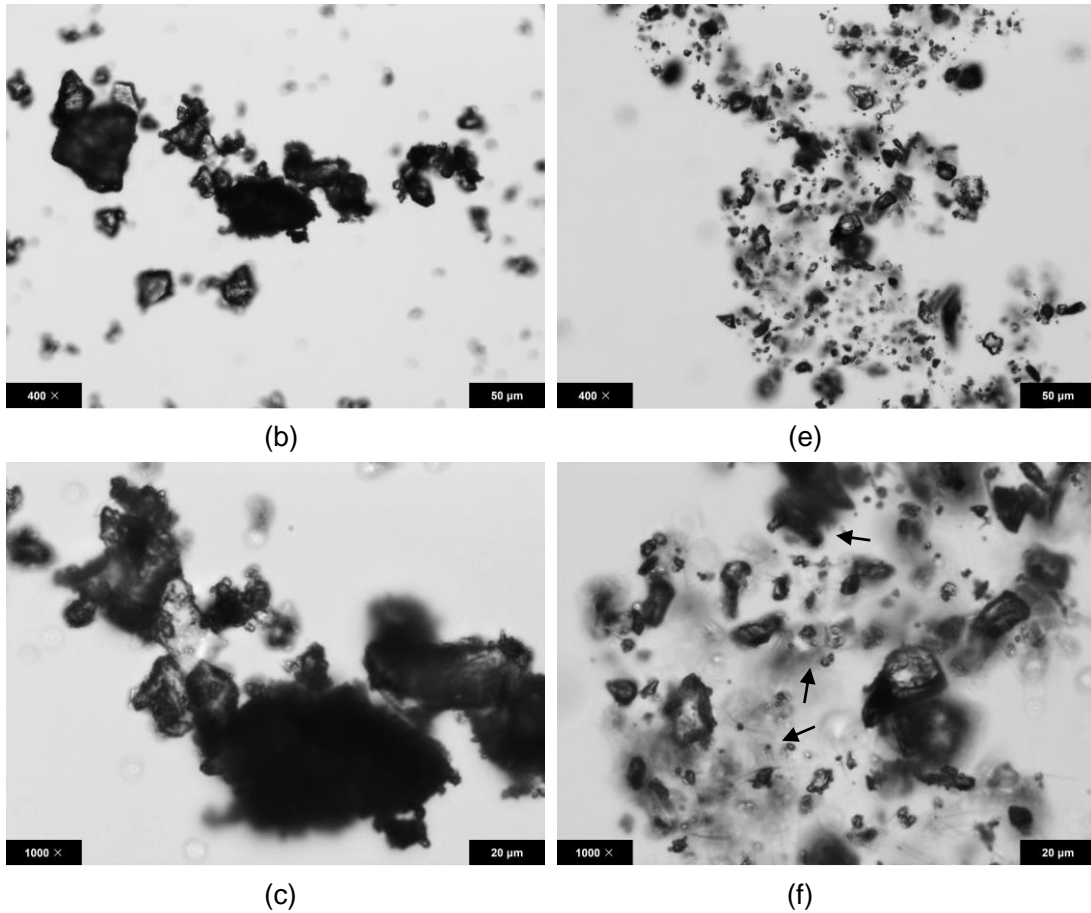
316 may facilitate the dissolution of mineral phases and hydration of cement, and hence
317 influences the agglomeration of cement particles. The structural organization of cement
318 particles in C-EW system is presented in Fig. 6(a)-6(c). Flocculated structures with larger
319 size than that in both C-W and C-E systems are observed in C-EW system. The severer
320 flocculation in C-EW system than that in C-E system should be caused by the enhanced
321 dissolution of mineral phases and production of hydrates, which certainly produces more
322 charges on surface of cement particles. On the other hand, when we compare the C-EW
323 system with C-W system, the ion strength of the medium in C-EW system must be lower than
324 that in C-W system, because of the less dissolution of mineral phases in C-EW system than
325 in C-W system. We believe that the lowered ion strength of the medium in C-EW system
326 should be responsible for the larger flocculated structures than in C-W system. The mean
327 particle size of C-EW system ascends to 9.40 μm from the 8.09 μm of C-W system and 4.59
328 μm of C-E system. Meantime, the decreases of circularity and Dpd to 0.80 and 1.51 indicate
329 that the dispersion degree of particles is lowest in the mixture medium.



330
331

(a)

(d)



332
333

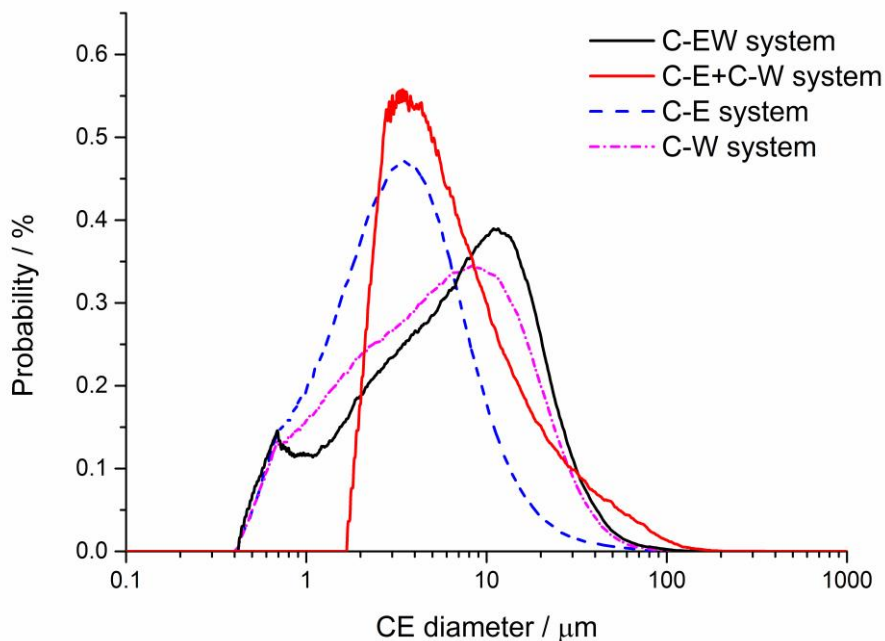
334
335

336 Fig. 6 Images of organization structure of cement particles in C-EW system (a)(b)(c) and C-
337 E+C-W system (d)(e)(f)

338

339 Different from being dispersed in the new type dispersion medium of ethanol solution (C-EW
340 system), cement particles may form a distinctive structural organization if C-W system
341 containing flocculated structures is mixed with C-E system with large amount of individual
342 particles. By mixing the C-W system and C-E system with the mass ratio of 1:1, C-E+C-W
343 system was obtained, whose mesostructure is displayed in Fig. 6(d)-6(f). A unique woolly
344 cloudlike aggregation is observed in C-E+C-W system. Specifically, the aggregation structure
345 contains two parts, the main body that is formed by a variety of flocculated particles and a
346 covering layer of individual tiny particles, respectively corresponding to the typical structures

347 in C-W system and C-E system. That is to say, the organization of cement particles in C-
348 E+C-W system is simply a mixture of that in C-E system and C-W system whereas cement
349 particles in ethanol solution (C-EW system) form flocculated structures with larger size than
350 that in both C-W and C-E systems. The difference between the morphologies of C-EW and
351 C-E+C-W systems may be associated with the changes in the zeta potential of cement
352 particles in different dispersion mediums. In the particle size distribution curve of C-E+C-W
353 system (Fig. 7), large particles with size of 30~300 μm are found. Consequently, the mean
354 particle size increases to 10.12 μm and Dpd decreases to 1.51 due to the appearance of
355 aggregations, indicating a bad dispersion state of cement particles in C-E+C-W system.



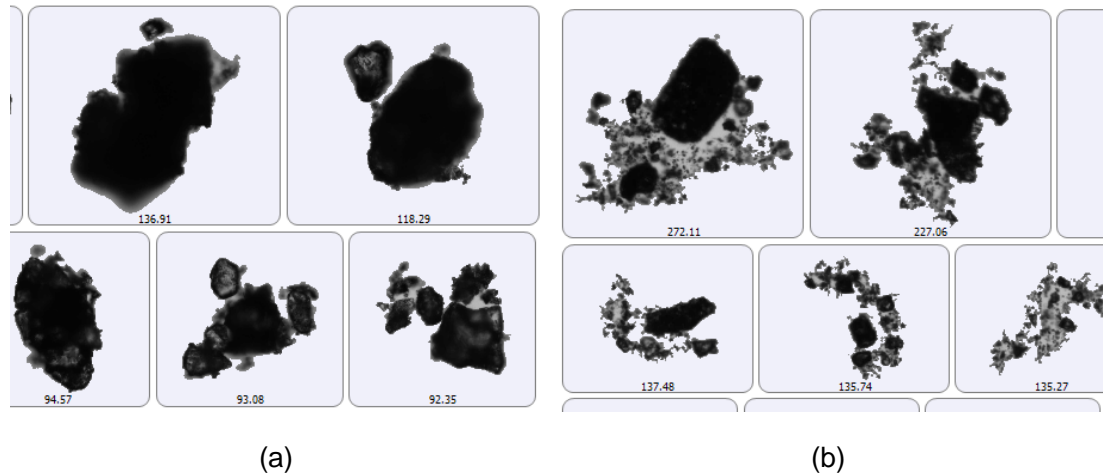
356

357 Fig. 7 Comparisons of particle size distribution of C-EW, C-E+C-W, C-E and C-W systems

358

359 Figure 8 provides some typical images of large particles in C-EW and C-E+C-W systems

360 extracted by the image analytical software, in which the grey particles are supposed to be
361 the adsorbed water and the entrapped water while the black ones are the cement particles.
362 The significant variations on the granular morphology of the two systems could be clearly
363 seen.



364
365 (a) (b)
366 Fig. 8 Typical morphology and CE diameter of particles in C-EW system (a) and C-E+C-W
367 system (b) (μm)

368
369 In summary, the results presented above indicate that this analytical approach using
370 Morphologi G3 is a suitable technique to identify and differentiate the varied mesostructural
371 organization of cement particles in different dispersion mediums in term of particle size,
372 granular shape and fractal dimension of spatial distribution. It has been observed that S-S
373 structure and L-S structure are the main dispersed phases in C-A system due to the huge
374 surface energy of small particles and the existence of instinct charges on cement surface.
375 Ethanol, an inert and good dispersion medium, enables cement particles to present majorly
376 individual particles and a small amount of L-S structures. There is a large quantity of
377 flocculated structures in C-W system caused by the strong electrostatic interactions among

378 cement particles stemming from the dissolution of mineral phases and initial hydration of
379 cement. Flocculated structures with larger size are observed in C-EW system, while in the
380 case of C-E+C-W system, a unique woolly cloudlike association agglomeration structure is
381 observed. Based on the three structural parameters, it is found that the dispersion degree of
382 cement particles in these mediums is in the order of C-E > C-A > C-W > C-EW > C-E+C-W.

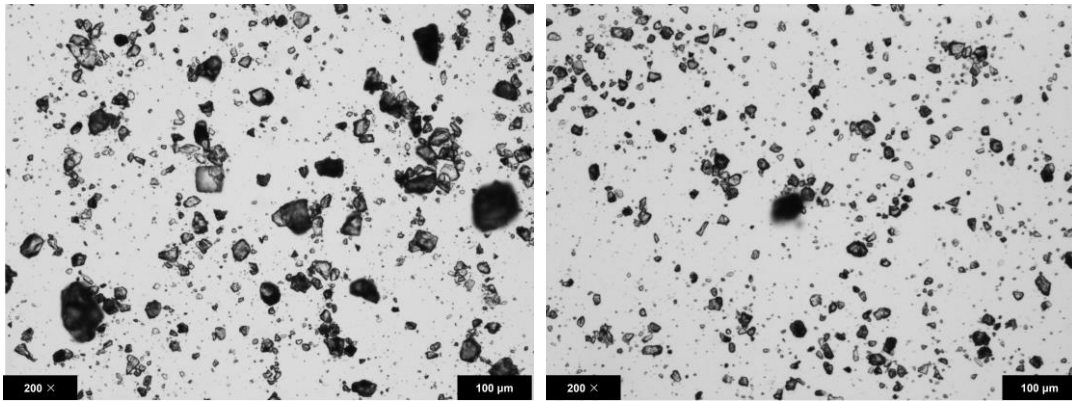
383

384 3.2. Influences of superplasticizers on mesostructure of FCP

385 It has been well accepted that the addition of superplasticizers in cement pastes destroys the
386 flocculated structure of cement particles in cement pastes and thus leads to enhanced
387 dispersion of cement particles, due to the generation of electrostatic repulsion and/or steric
388 hindrance between cement particles [9, 10]. It is possible to visualize and quantify the
389 influences of the superplasticizer on the mesostructure of cement pastes by comparing the
390 granular images and the structural parameters of the cement pastes containing
391 superplasticizer with those of the reference cement paste, in which a great number of
392 flocculated structures are observed with the mean particle size of 8.09 μm and the Dpd of
393 1.68 as water is used as the dispersion medium. Indeed, the incorporation of superplasticizer
394 causes a significant change on the granular morphology, agglomerates and the spatial
395 distribution as shown in Fig. 9-10.

396

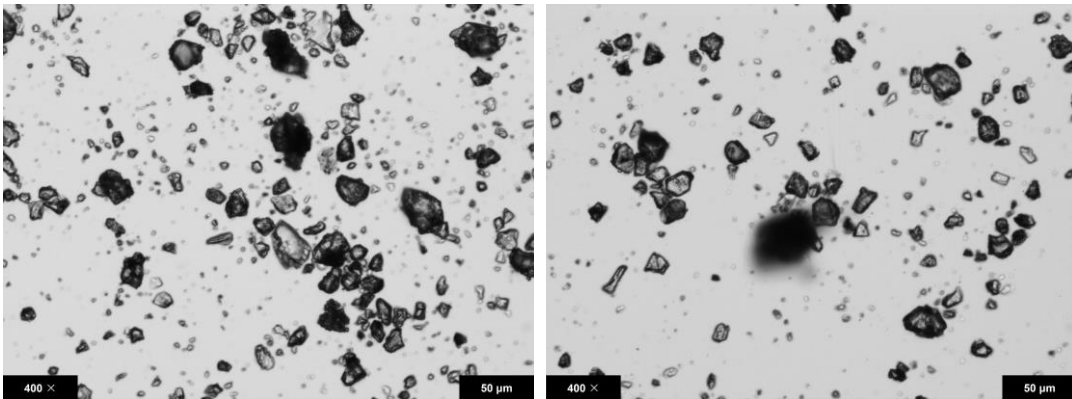
397
398



(a)

(d)

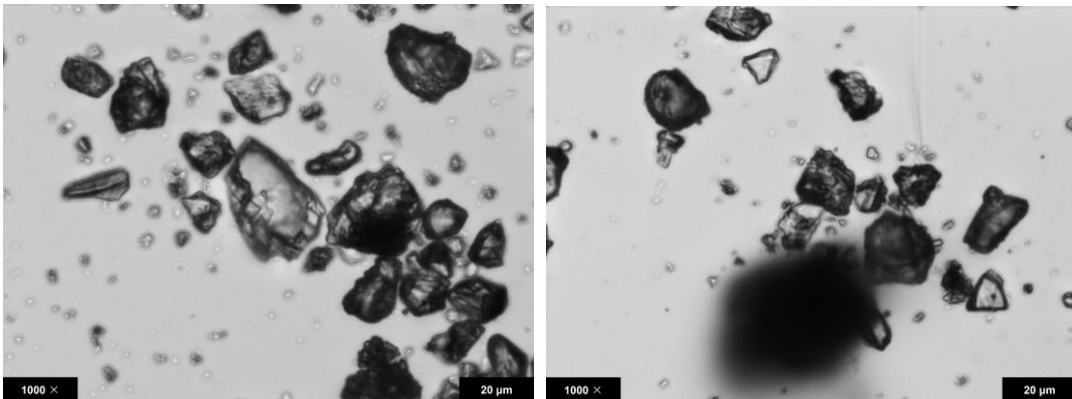
399
400



(b)

(e)

401
402



(c)

(f)

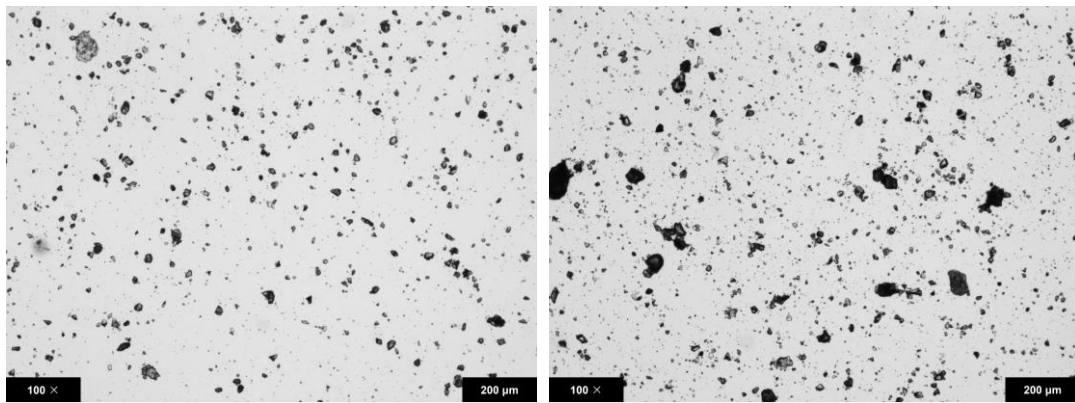
403 Fig. 9 Images of organization structure of cement particles in C-W-P0.1 system (a)(b)(c)

404

and C-W-P0.3 system (d)(e)(f)

405

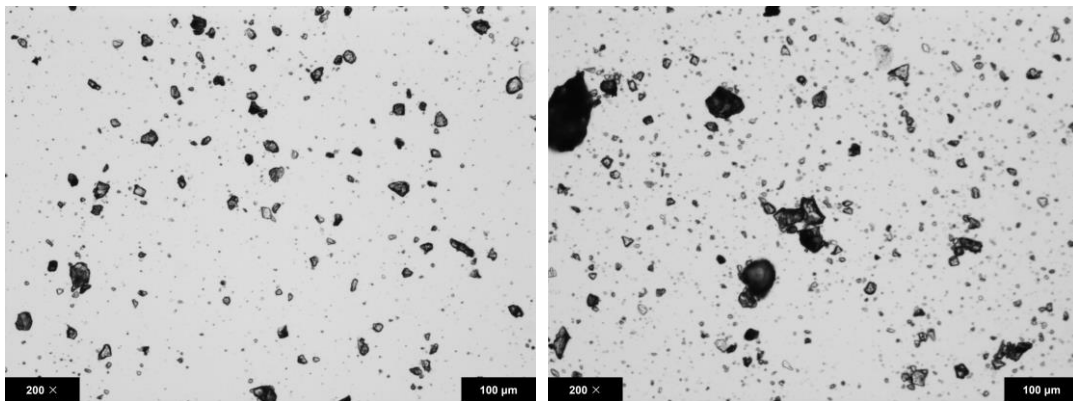
406
407



(a)

(d)

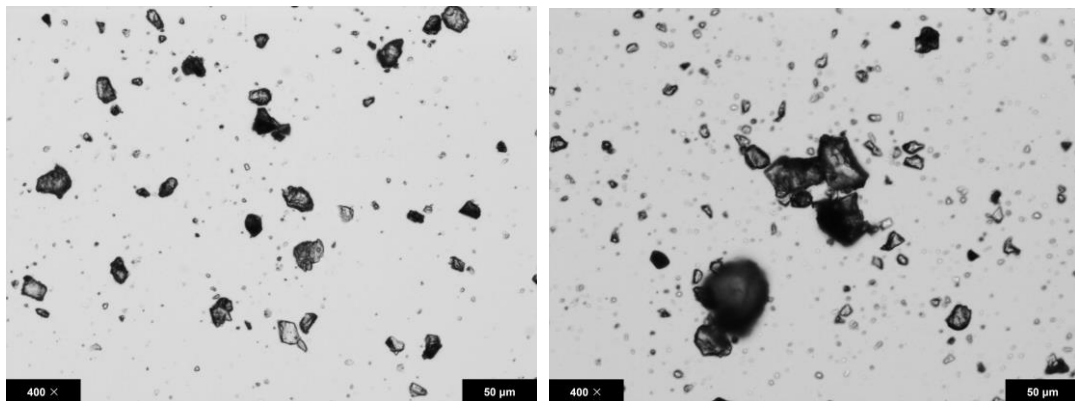
408
409



(b)

(e)

410
411



(c)

(f)

412 Fig. 10 Images of organization structure of cement particles in C-W-P0.5 system (a)(b)(c)
413 and C-W-N0.5 system (d)(e)(f)

414

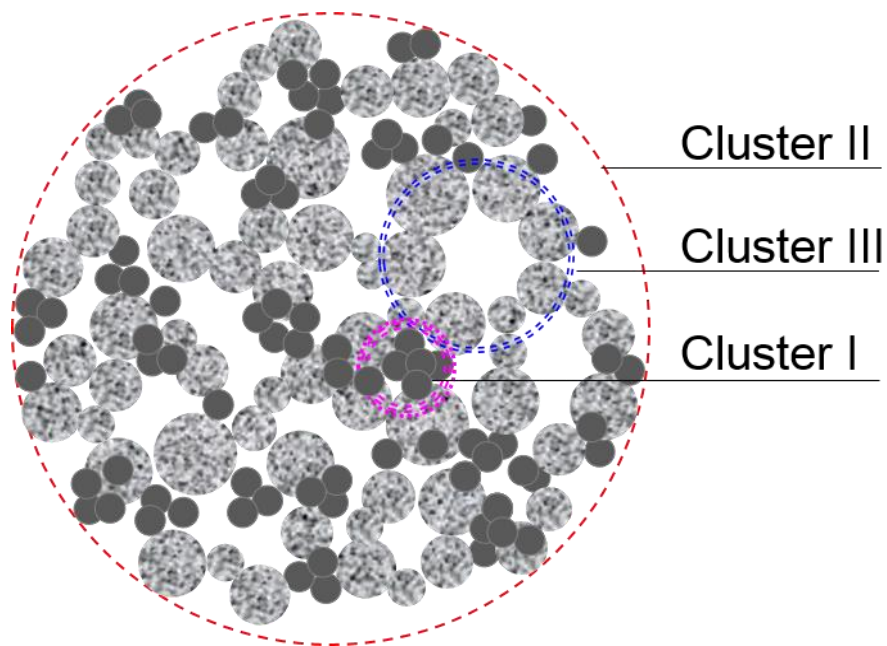
415 Most of the cement particles with clear edges and hard corners, associated with some
416 flocculated structures, are well dispersed under the influence of the superplasticizer. The

417 structural organization of cement particles depends on the superplasticizer amount and type.
418 Higher superplasticizer dosage brings about flocculated structures with smaller size and
419 evidently reduces their amounts in the meantime. In the dispersion medium of aqueous
420 solution with PCE mass concentration of 0.5%, polygon crystals are present in greater
421 numbers and small flocculated structures almost disappear, as shown in Fig. 10(a)-10(c). On
422 the other hand, in the aqueous solution with NSF mass concentration of 0.5%, small
423 flocculated structures are always visible regardless of the dosage of NSF, which may stem
424 from the different dispersion capability of PCE and NSF. It has been well documented that
425 the dispersing capability of PCE is stronger than that of NSF, and hence PCE allows much
426 better dispersion of cement particles in aqueous medium [1, 27] at the same dosage. Limited
427 by the dispersion capability, NSF is less effective to disassemble the strongly bonded
428 flocculated structures.

429

430 On the basis of the granular characteristics shown in Fig. 9-10, the flocculated structures
431 could be roughly sorted into three groups (classes) according to the level of difficulty to be
432 disassembled, which are denoted cluster I, II, and III from small to large order. Factually, the
433 division of the flocculated structures is closely dependent on the bonding forces between
434 particles. It is seen from the micrograph that the cement particles are mainly composed by
435 small particles of 1-10 μm (S), medium particles of 10-30 μm (M) and large particles of 30-
436 100 μm (L), in which small particles tend to agglomerate together to form S-S structure due
437 to their huge specific surface energy and could be broken apart easily in the presence of a

438 low dosage of superplasticizer, namely cluster I structure. On the contrary, large particles
439 with strong electrostatic interactions form L-L structure and are hard to be dispersed, i.e.,
440 cluster III structure. The rest of particles constitutes S-M-L structure corresponding to cluster
441 II structure, as shown in Fig. 11. Obviously, the interaction forces between the particles are
442 in the order of $F_{S-S} < F_{S-M-L} < F_{L-L}$. Thus, superplasticizers are able to disassemble different
443 flocculated structures depending on their types and dosages, thereby presenting distinct
444 plasticizing effects. Superplasticizers with stronger dispersing capability facilitate the
445 disassembly of more strongly bonded flocculated structures, thereby increasing the
446 flowability of FCP more significantly.



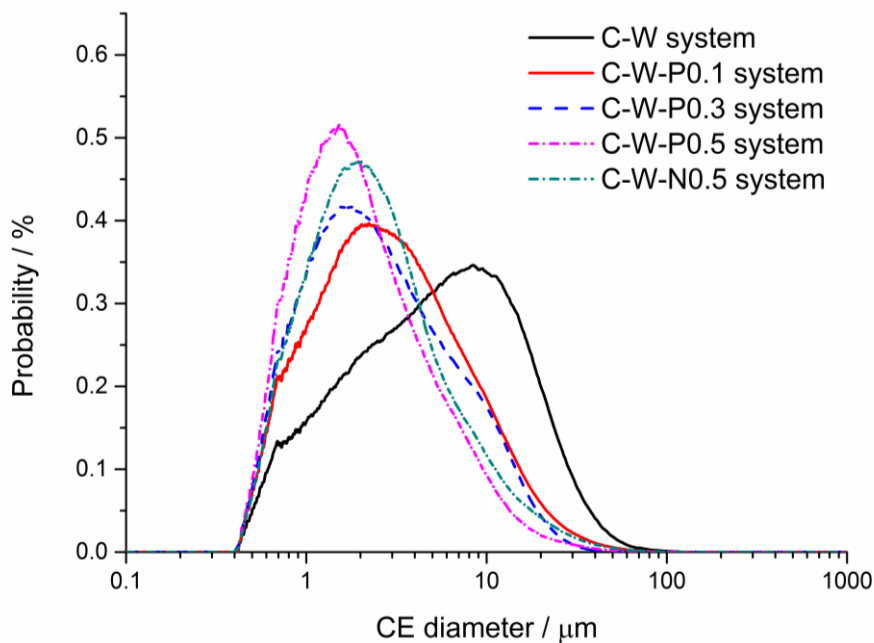
447

448 Fig. 11 Schematic illustration of flocculated structure of cement particles

449

450 From a quantitative point of view, the variations of the three structural parameters reflect the
451 influence of superplasticizers on the mesostructure of fresh cement paste. The particle size
452 distribution curves of the cement pastes containing different superplasticizers are presented

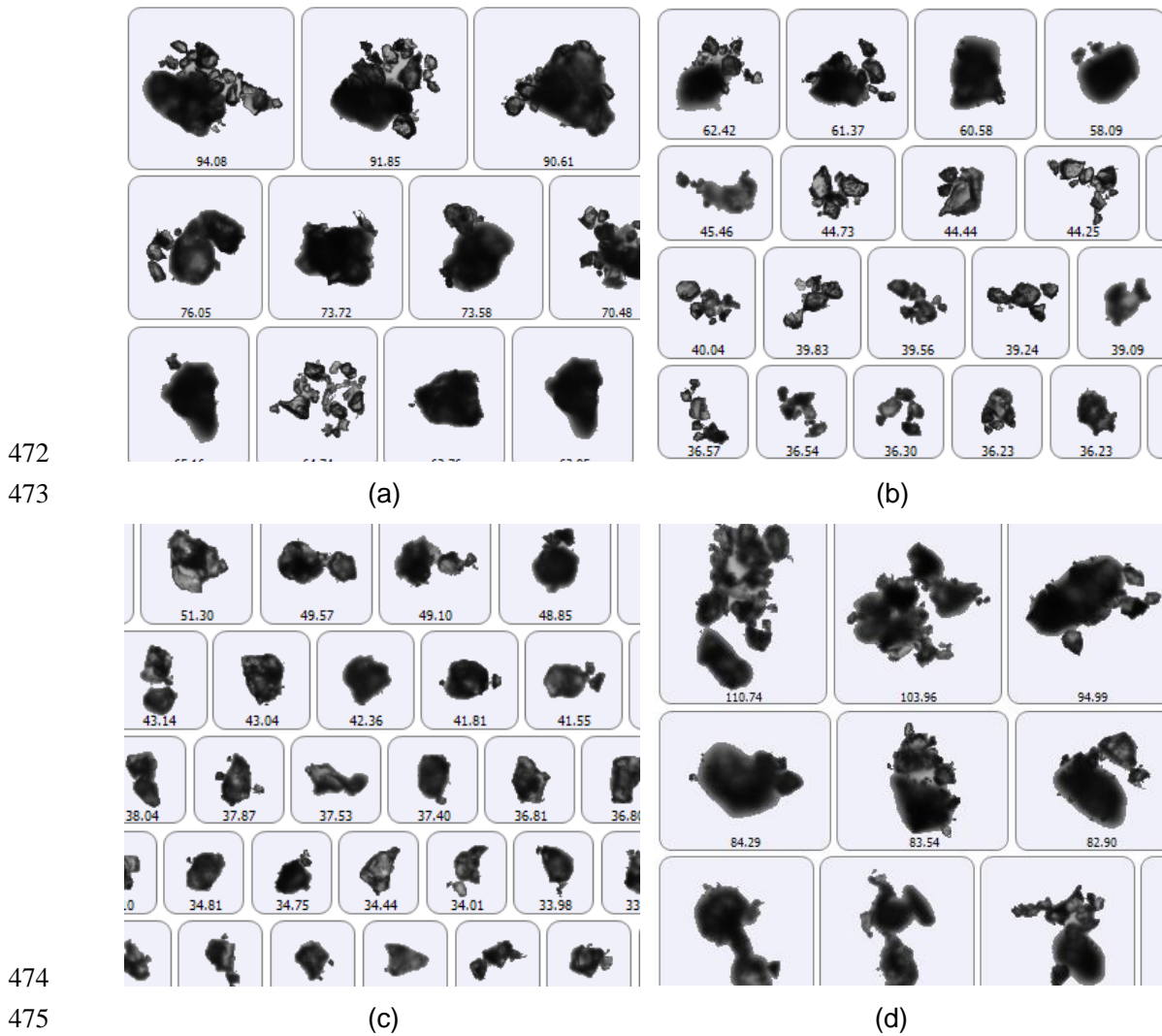
453 in Fig. 12. It is noticed that the incorporation of superplasticizers leads to a notable left shifting
454 of particle size distribution due to the decrease in the amount of large particles and the
455 marked increase in small particles content. In such way, with the increase of superplasticizer
456 concentration, the mean particle size decreases to 2.99 μm in C-W-P0.5 system from the
457 8.09 μm of C-W system while the circularity and Dpd rise to 0.89 and 1.94 from the original
458 0.83 and 1.68 in C-W system respectively, suggesting the superior dispersion state of cement
459 particles in the aqueous medium with PCE superplasticizer. In comparison, C-W-N0.5 system
460 displays a relatively inferior dispersion state indicated by the mean particle size of 3.71 μm
461 and the Dpd of 1.86.



462
463 Fig. 12 The influence of superplasticizers on the particle size distribution of fresh cement
464 pastes

465
466 Similarly, some typical images of large particles in C-W-P and C-W-N systems are presented

467 in Fig. 13, where the significant variations of the structural organization depending on the
 468 types and concentrations of superplasticizers could be apparently observed. The high-quality
 469 images associated with the variations in particle size and shape as well as spatial distribution
 470 provide straightforward information on the mesostructure of FCP, which is essential for
 471 understanding the working mechanism of superplasticizers.



474

475

476 Fig. 13 Typical morphology and CE diameter of particles in C-W-P and C-W-N systems

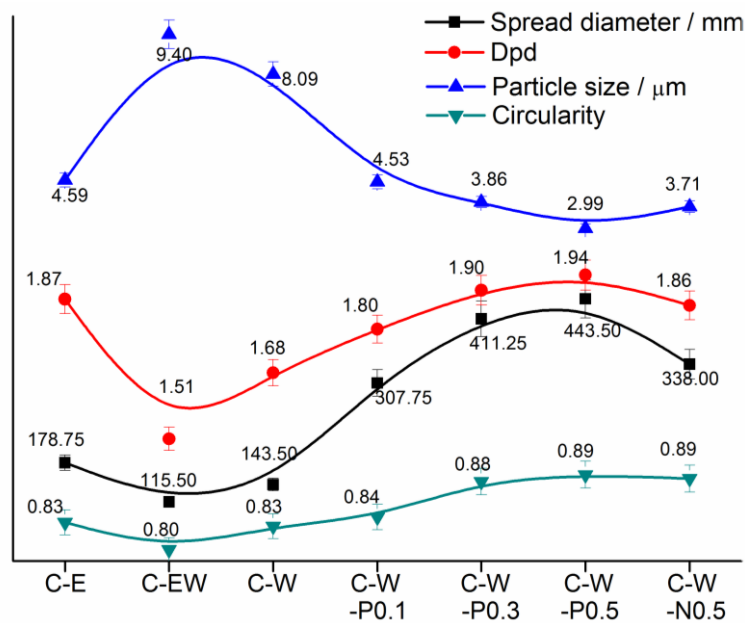
477 (μm) (a) C-W-P0.1 system; (b) C-W-P0.3 system; (c) C-W-P0.5 system; (d) C-W-N0.5

478 system

479

480 3.3. Correlation of mesostructure with rheological behavior

481 The rheological behaviors of fresh cement pastes are usually characterized by the spread
 482 diameter according to the fluidity test [27, 28]. By comparing the fluidity curve of FCPs with
 483 the curves of the three structural parameters corresponding to different suspension systems,
 484 (Fig. 14), it is interesting to see that the curves of Dpd and circularity behave in much the
 485 same way as the fluidity curve. Contrary to them, the mean particle size curve shows an
 486 inverted variation trend to the fluidity curve. That is to say, higher fluidity corresponds to larger
 487 Dpd and circularity as well as a lower mean particle size. Moreover, mean particle size and
 488 Dpd are more sensitive to indicate the change of the fluidity of FCP.



489

490 Fig. 14 The variations of fluidity and structural parameters of fresh cement paste in different
 491 dispersion mediums

492

493 The comparison between the structural parameters and the fluidity of the FCP in varied
 494 mediums allows a better understanding of the real granular morphology in varied dispersion

495 mediums and the influences of superplasticizers on the dispersion state of cement particles,
496 and thus the mesostructural organization of cement particles in the pastes. In this way, the
497 connection between the mesostructure and the macroscopic rheological properties is
498 established through the structural parameters.

499

500 **4. Conclusions**

501 In this paper, for the first time, comparative study on the mesostructure of diluted FCPs with
502 different dispersion mediums was carried out using Morphologi G3 with the aim of
503 characterizing the organization of cement particles in the FCP at a mesoscopic scale and
504 establishing the correlation of mesostructure with macroscopic rheological properties. On the
505 basis of the results above, the following conclusions can be drawn:

506 (1) Morphologi G3 with high sensitivity and high resolution is a powerful tool to identify and
507 differentiate the structural organization of cement particles dispersed in different
508 mediums by providing high-quality images associated with structural parameters. Three
509 structural parameters including particle size, granular shape and fractal dimension of
510 particle spatial distribution (D_{pd}) allow to quantitatively characterize the organization of
511 cement particles in fresh cement pastes at a mesoscopic scale.

512 (2) The association of the small particles (S-S structure) and the agglomeration of the small
513 particles sticking to the larger ones (L-S structure) are the main dispersed phases in C-
514 A system. Cement particles present majorly individual particles and a small amount of L-
515 S structures in C-E system. There is a large quantity of flocculated structures in C-W

516 system caused by the quick dissolution of mineral phases as well as hydration.
517 Flocculated structures with larger size are observed in C-EW system while in the case of
518 C-E+C-W system, a unique woolly cloudlike association agglomeration structure is
519 observed. Based on the three structural parameters, it is found that the dispersion degree
520 of cement particles in these mediums is in the order of C-E > C-A > C-W > C-EW > C-
521 E+C-W.

522 (3) In the presence of superplasticizer, most of the cement particles with clear edges and
523 hard corners, associated with some flocculated structures, are well dispersed. With the
524 increase of superplasticizer concentration, the mean particle size decreases while both
525 of the circularity and Dpd rise. According to the level of difficulty to be disassembled, the
526 flocculated structures were roughly sorted into three classes from small to large order,
527 i.e., cluster I, II, and III, corresponding to S-S structure, L-M-S structure and L-L structure
528 respectively.

529 (4) The relationship between the mesostructural organization of cement particles in a fresh
530 cement paste and its rheological behavior is established by employment of the three
531 structural parameters. Higher fluidity corresponds to larger Dpd and circularity as well as
532 a lower mean particle size. Moreover, the mean particle size and Dpd are more sensitive
533 to indicate the change of the fluidity of fresh cement paste.

534

535 **Acknowledgement**

536 The financial supports from the National Natural Science Foundation of China (Grant No.

537 51173094 and U1301241) and the Fundamental Research Funds for the Central Universities
538 (No. 2016JBM036) are gratefully acknowledged.

539

540 **References**

541 [1] Rubio-Hernández F J, Velázquez-Navarro J F, Ordóñez-Belloc L M. Rheology of
542 concrete: a study case based upon the use of the concrete equivalent mortar. *Materials*
543 *and structures*, 2013, 46(4): 587–605.

544 [2] Sun Z, Voigt T, Shah S P. Rheometric and ultrasonic investigations of viscoelastic
545 properties of fresh Portland cement pastes. *Cement and Concrete Research*, 2006,
546 36(2): 278–287.

547 [3] Roussel N. A thixotropy model for fresh fluid concretes: theory, validation and application.
548 *Cement and Concrete Research*, 2006, 36(10): 1797–1806.

549 [4] Barnes H A, Hutton J F. *An introduction to rheology*. Elsevier, 1989.

550 [5] Saak A W, Jennings H M, Shah S P. The influence of wall slip on yield stress and
551 viscoelastic measurements of cement paste. *Cement and concrete research*, 2001,
552 31(2): 205–212.

553 [6] Sakai E, Kasuga T, Sugiyama T, et al. Influence of superplasticizers on the hydration of
554 cement and the pore structure of hardened cement. *Cement and concrete research*,
555 2006, 36(11): 2049–2053.

556 [7] Plank J, Hirsch C. Impact of zeta potential of early cement hydration phases on
557 superplasticizer adsorption. *Cement and Concrete Research*, 2007, 37(4): 537–542.

- 558 [8] Yoshioka K, Tazawa E, Kawai K, et al. Adsorption characteristics of superplasticizers on
559 cement component minerals. *Cement and Concrete Research*, 2002, 32(10): 1507–
560 1513.
- 561 [9] Plank J, Sachsenhauser B. Experimental determination of the effective anionic charge
562 density of polycarboxylate superplasticizers in cement pore solution. *Cement and*
563 *Concrete Research*, 2009, 39(1): 1–5.
- 564 [10] Winnefeld F, Becker S, Pakusch J, et al. Effects of the molecular architecture of comb-
565 shaped superplasticizers on their performance in cementitious systems. *Cement and*
566 *Concrete Composites*, 2007, 29(4): 251–262.
- 567 [11] Zingg A, Winnefeld F, Holzer L, et al. Adsorption of polyelectrolytes and its influence on
568 the rheology, zeta potential, and microstructure of various cement and hydrate phases.
569 *Journal of Colloid and Interface Science*, 2008, 323(2): 301–312.
- 570 [12] Lilkov V, Dimitrova E, Gaidardzhiev S. Microscopic and laser granulometric analyses of
571 hydrating cement suspensions. *Cement and concrete research*, 1999, 29(1): 3–8.
- 572 [13] Zingg A, Holzer L, Kaech A, et al. The microstructure of dispersed and non-dispersed
573 fresh cement pastes-new insight by cryo-microscopy. *Cement and Concrete Research*,
574 2008, 38(4): 522–529.
- 575 [14] Han S, Yan P Y, Kong X M. Study on the compatibility of cement-superplasticizer system
576 based on the amount of free solution. *Science China Technological Sciences*, 2011,
577 54(1): 183–189.
- 578 [15] Autier C, Azema N, Taulemesse J M, et al. Mesostructure evolution of cement pastes

- 579 with addition of superplasticizers highlighted by dispersion indices. Powder Technology,
580 2013, 249: 282–289.
- 581 [16] Felekoğlu B. Effects of PSD and surface morphology of micro-aggregates on admixture
582 requirement and mechanical performance of micro-concrete. Cement and Concrete
583 Composites, 2007, 29(6): 481–489.
- 584 [17] Masad E, Muhunthan B, Shashidhar N, et al. Internal structure characterization of
585 asphalt concrete using image analysis. Journal of computing in civil engineering, 1999,
586 13(2), 88–95.
- 587 [18] Felekoglu B. A new approach to the characterisation of particle shape and surface
588 properties of powders employed in concrete industry. Construction and Building
589 Materials, 2009, 23(2): 1154–1162.
- 590 [19] Paumier S, Pantet A, Monnet P. Evaluation of the organization of the homoionic smectite
591 layers (Na⁺ or Ca²⁺) in diluted dispersions using granulometry, microscopy and
592 rheometry. Advances in colloid and interface science, 2008, 141(1): 66–75.
- 593 [20] Autier C, Azéma N, Boustingorry P. Using settling behaviour to study mesostructural
594 organization of cement pastes and superplasticizer efficiency. Colloids and Surfaces A:
595 Physicochemical and Engineering Aspects, 2014, 450: 36-45.
- 596 [21] Wang L J, Huang F Y, Ma X C. Experimental research on the saturation point of
597 superplasticizers in cement based on fractal dimension. Journal of Wuhan University of
598 Technology, 2008 30(2): 28–31.
- 599 [22] Dexter A R. Advances in characterization of soil structure. Soil and tillage research, 1988,

600 11(3): 199–238.

601 [23] Cnudde V, Cwirzen A, Masschaele B, et al. Porosity and microstructure characterization
602 of building stones and concretes. *Engineering geology*, 2009, 103(3): 76–83.

603 [24] Yang X. Three-dimensional characterization of inherent and induced sand
604 microstructure. PhD Dissertation, Georgia Institute of Technology, 2005. 12.

605 [25] Muhua T, Roy D M. An investigation of the effect of organic solvent on the rheological
606 properties and hydration of cement paste. *Cement and Concrete Research*, 1987, 17(6):
607 983–994.

608 [26] Adamson A W, Gast A P. *Physical chemistry of surfaces*. 6th ed. John Wiley & Sons,
609 1967.

610 [27] Zhang Y, Kong X. Correlations of the dispersing capability of NSF and PCE types of
611 superplasticizer and their impacts on cement hydration with the adsorption in fresh
612 cement pastes. *Cement and Concrete Research*, 2015, 69: 1–9.

613 [28] Kong X, Zhang Y, Hou S. Study on the rheological properties of Portland cement pastes
614 with polycarboxylate superplasticizers. *Rheologica Acta*, 2013, 52(7): 707–718.